Towards a production-line classification of metallic satin-finished surfaces using coherent light

Yuri López de Meneses[a], Grégoire Meylan, Florent Monay, Jacques Jacot[a]

[a]LPM–Institut de Production et Robotique–EPFL, Switzerland

ABSTRACT

Some manufacturing processes, such as satin finish on stainless steel parts for the watchmaking and biomedical industries, apply purely aesthetic, global criteria for their quality control. This control is currently performed by human operators, and is found to be subjective, due to variability in operator judgement. This project aims to develop a device for automatic, production-line classification of satin finish according to the aesthetic criteria currently applied in the watchmaking industry. We exploit two coherent light phenomena to produce features to classify the parts into the same classes indicated by human operators. The analysis of the optical Fourier transform and the scattering pattern are used to generate high-dimensional feature vectors for their subsequent classification. The vectors, corresponding to different regions of the part surface, are classified using Principal Component Analysis and Kohonen networks. Experimental results show that both optical phenomena provide features capable of discriminating between conforming and nonconforming parts. Classification is simple enough to afford an inspection in under 1 s and its robustness has also been verified. We have thus completed a first step towards a simple, production-line device capable of providing an automatic, objective evaluation based on aesthetic quality criteria.

Keywords: Classification, scattering, optical Fourier transform, aesthetic quality-control, satin finish on metal surface, Principal Component Analysis, Kohonen Neural Networks

1. INTRODUCTION

Many industrial inspection tasks are concerned with verifying the presence, position or orientation of a part or component or else verifying its dimensional conformity to given specifications. These tasks are usually automated using computer vision systems. Other inspection tasks verify the surface state of the parts, typically by testing their mechanical properties, and these are also highly automated. There is a type of inspection in between these two that has been hardly automated: aesthetic quality control. In the watchmaking, micromechanics, biomedical (implants) and jewelry industries parts have to conform to aesthetic criteria such as glitter, transparency, hue, etc.

This project deals with the inspection of the satin-finish operation on stainless steel parts in the watchmaking industry. The main physical attribute of satin-finished parts is the parallel, regular grooves that confer them a matte aspect. The parts are typically manufactured by brushing a prepolished, metal surface with a diamond-embedded rotating brush. The quality of the part depends on the surface state of the prepolished parts, on the brush wear, the pressure applied on the part, the duration of the brushing as well as the dexterity of the operator –in the luxury watchmaking industry this processes is usually carried out manually.

Inspection is currently performed manually by specially-trained human operators. Therefore their evaluation is qualitative, even subjective as fatigue and external psychological factors induce a great intra- and interoperator variability. The ultimate goal of this project is to build a portable device for the online, contactless characterization of parts based on their surface appearance. This device should provide an objective, repeatable and quantitative evaluation of the part. To this end we have exploited two coherent-light phenomena to provide us with features to classify the pieces according to the classes defined by the human inspectors.

Further author information: (Send correspondence to Yuri L. de Meneses.)
Yuri L. de Meneses: E-mail: yuri@ieee.org, Telephone: +41 21 693 3908 Laboratoire de Production Microtechnique (LPM) – Institut de Production et Robotique (IPR), Ecole Polytechnique Fédérale de Lausanne (EPFL), 1015 Lausanne, Switzerland
Jacques Jacot: E-mail: jacques.jacot@epfl.ch, Telephone: +41 21 6933908

This paper is organized as follows. In section 2 we describe the classification methodology, which is common to both methods. The fisrt method, based on the optical-domain Fourier transform is discussed in section 3. Section 4 deals with scattering as a surface-characterization method. The paper is completed with a conclusion that sums up the results and compares them.

2. METHODOLOGY

The two systems for the classification of satin-finished parts that we have developped employ the same classification methodology, which we describe in this section.

The goal of the classification is to categorize the parts into several classes – at least two: conforming and nonconforming, but the last one can be divided into subclasses according to different assignable causes of the defects – and this classification has to correspond to the one given by the human operators.

If the actual criteria employed by the human operators were known, their classification could be easily reproduced. Unfortunatelly, although human operators undergo a training phase to define and standardize their decision criteria, these are not sufficiently formalized and do not have a sufficiently quantitative nature to be used by a computer. Therefore we have used new, artificial criteria and we have tried to match the cathegories thus obtained to the ones defined by the human operators.

The criteria used for classification are based on some quantitative characteristics of the parts, called *features*. Because of the complexity of the problem a single feature is not sufficient, we will need to use several of them that we will group into a *feature vector*. Thus, each part or rather, each inspected area of the part has an associated feature vector.

Classification consists in assigning to each feature vector a class out of a given set of possible classes. To do so, classifiers function on the principle that similar inputs , i.e. belonging to the same class, should have feature vectors that are close to each other. The classifier operates on vectors and is completely unaware of the physical meaning of the features or vector components. These can be light intensities in one case and spatial-frequency power-density in another. Hence classifiers are generic algorithms that can be applied to different problems.

The process we have followed is schematized in figure 1. Images related to the parts under inspection are acquired as described in sections 3.2 and 4.1. Next several features are extracted from the images (cf. sections 3.3 and 4.2) to form the feature vectors. These features are based on the properties of coherent light reflecting upon the satin-finished, metallic surface of the parts. In some cases features may undergo a dimension-reduction stage (cf. section 2.1) before training the classifier (section 2.2). The feedback loop indicates that if the training is unsuccesful, new features should be sought and the process started again.

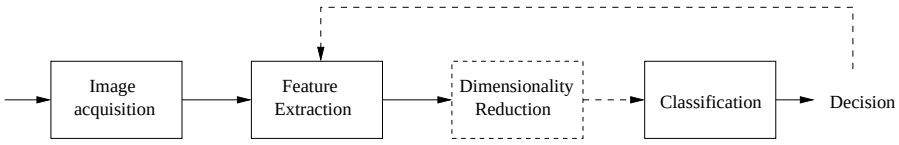

Figure 1. Classification process: Images related to the parts under inspection are acquired and features are extracted from them to form the feature vectors. In some cases features may undergo a dimension-reduction stage before training the classifier. If the training is unsuccesful, the process should be started again with different features.

2.1. Dimension reduction with PCA

In some cases feature vectors can be very high-dimensional. This complicates the classification tasks because the amount of data can be overwhelming – the time it takes the classifier to learn increases with the dimension – and because many features can turn out to be useless, thus introducing noise into the system. To limit these problems, in some cases we have added a dimension-reducing step, shown in dashed lines in figure 1.

Principal Component Analysis (PCA)[1] has been used for dimensionality reduction. It is a statistical tool that computes the linear transformation (linear combinations of vector components) that preserves most of the variance of the input

distribution and eliminates the rest. The rationale behind it is that components (and their linear combinations) that have low variance do not provide enough information and that furthermore this variance could be due to measurement noise.

This allows us to start from a high number of features, even "wild guesses" and then, by using the PCA, select the most relevant feature combinations.[2,3] It is even possible to further simplify these combinations by identifying the individual features that have the highest participation (called *loading*) in the combination. The exact procedure is thoroughly discussed in.[4]

Because the transformation is linear –it actually provides a rotation matrix– dimensionality reduction is a very fast operation. However, since the transformation has to be orthogonal[1] its performance is degraded for data that do not lie along straight, orthogonal directions.

If the input vectors are reduced to 2 or 3 dimensions, the resulting distribution can be easily visualized and, if it shows distinguishable clusters of data belonging to a similar class then in most cases it is possible to manually define the borders among classes. As we will show in sections 3.4 and 4.3, in most cases this manual classification is sufficient.

2.2. Classifiers

The last step in the process is applying the actual classifier. Besides the *manual classification* described in section 2.1 we have used Self Organized Maps (Kohonen networks)[5] and Learning Vector Quantization (LVQ)[1,6] to automatically classify the data and test the robustness of the classification by introducing new, different data.

Kohonen networks, in their 2D version, try to cover the N-dimensional input distribution by unfolding a grid of neurons that best approximate (in the least squares sense) the input data. They can be thought as a non-orthogonal version of the PCA. As the latter, Kohonen networks are unsupervised algorithms, that is, they do not require to know to which classes the input data belong. Rather, they try to find the "natural classes" in the distribution (as long as they exist). In our case it is necessary to verify afterwards that these natural classes correspond with the classification given by the human operators.

LVQ, on the other hand, is a supervised classification algorithm based on Kohonen maps. It requires that the training data be labeled with the class they belong to. Because it has this additional information regarding the classes, LVQ can provide a better classification than unsupervised systems do. However, it can not find more classes than the ones given during training.

3. OPTICAL FOURIER FEATURES

The regular grooves of the satin finish confer a certain periodic structure to the parts. Indeed, a test we had conducted with an optical profilometer[7] had shown that the grooves had a typical periodicity of $10\ \mu m$. We have therefore explored the use of this periodicity, as spatial-frequency features, to distinguish the types of satin-finish.

The Fourier transform of an image of the parts provides these features. To render the process faster, we have opted to perform the Fourier transform in the optical domain.

3.1. Optical Fourier Transform

The Fourier transform can be obtained in the situation depicted in figure 2. A source of coherent, monochromatic light projects a plane wave on a grid or similar intensity-modulation pattern on plane Σ_1. A lens (L_1) focuses the image of the pattern on the image plane Σ_3, which is beyond the focal plane of the lens Σ_2.

The scalar field in Σ_2, U_2, is proportional to the Fourier transform of the modulation $m(\vec{r})$ in plane Σ_1 and a phase term,[8,9] as in eq. 1.

$$U_2 = \left(-\frac{i}{\lambda \vec{OS}} \cdot U_0 \cdot e^{ik\vec{OS}} \cdot e^{-i\pi \frac{r_d^2}{\lambda \vec{OS}}} \right) \cdot \tilde{m}(\vec{\omega}) \tag{1}$$

A light-intensity detector, such as a CCD camera, placed in plane Σ_2 would record the intensity $I = U_2 \cdot U_2^* \propto |\tilde{m}(\vec{\omega})|^2$. Therefore, the image taken by the camera is proportional to the square magnitude of the spatial-frequency spectrum of the modulating pattern $m(\vec{r})$.

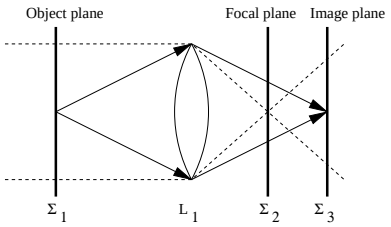

Figure 2. A thin lens can perform the Fourier transform in the optical domain

3.2. Setup

The principle outlined above has already been used in industrial inspection, but mostly for transmissive objects or materials.[10,11] For this project we have used a finite distance, reflective version of the setup shown in figure 2. Compared to the afocal setup, it requires a single lens and affords to illuminate larger surfaces.[12]

A diagram and picture of our setup is shown in figure 3. An almost plane wave is generated by coupling a 632.8 nm He-Ne laser to a 4 μm-diameter optical fiber, thus creating a point source. A large diameter lens (48 mm) focuses the laser light on the part under test, creating an elliptical spot of 16 x 8 mm^2. The reflected light is projected on a white screen and a CCD camera at 350 mm from it takes a picture of the intensity pattern.

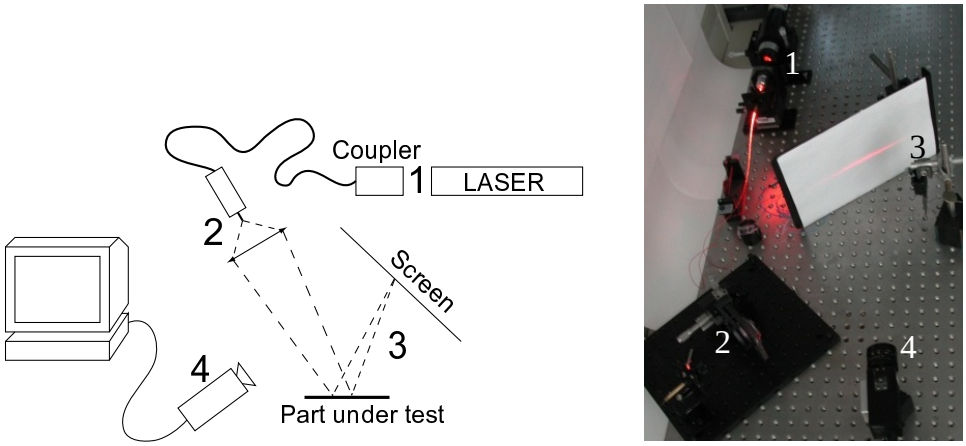

Figure 3. Setup for the optical Fourier transform

Because the parts under inspection have a microstructure –the grooves– and we are using coherent light, scattering appears, and the resulting image is not exactly the Fourier transform of the modulation function. Figure 4(a) shows the resulting images when inspecting a conforming and a nonconforming part. The light stripe indicates the presence of spatial-frequencies along only one direction.

3.3. Data

We have analyzed a batch of 7 flat, satin-finished parts: 3 conforming ones and 4 nonconforming ones, due to two different causes (a badly prepolished surface and a change of direction during brushing). From each part 9 different zones were sampled, therefore producing a total of 63 input vectors. Since the Fourier images (figure 4(a)) are mostly unidimensional we have taken the intensity profile along the stripe, as shown in figure 4(b).

The profile is centered on the brightest pixel (specular reflection spot) and it is 532 pixels long. To reduce noise in the profile and obtain a more comparable results we have applied a 5-pixel wide median filter. After filtering, the intensity profiles are directly used as feature vectors. Thus the input data are 63 vectors in a 532-dimensional space.

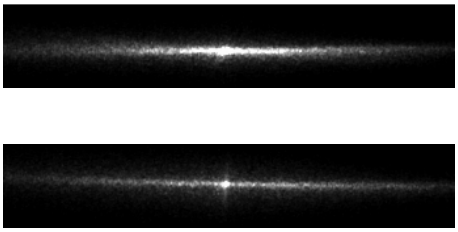

(a) Two images obtained with the optical setup. On top, a conforming part, below a nonconforming one.

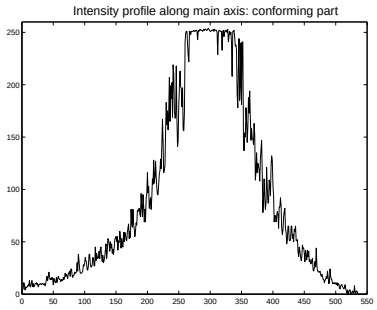

(b) Intensity profile along the stripe on the Fourier image, for a conforming part

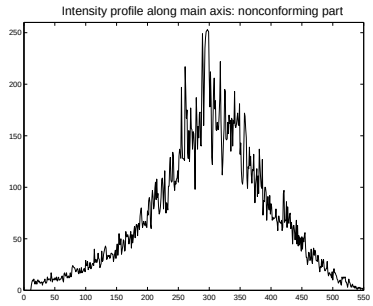

(c) Intensity profile for a nonconforming part

Figure 4. Optical-domain Fourier transform features

3.4. Results

We have performed a PCA (cf. section 2.1) and projected the vectors on their 2 principal components. The result is shown in figure 5a. The vectors form 3 clusters, but they are not perfectly separable, since conforming parts (x's) and some of the nonconforming parts (diamonds) are mixed. By selecting the 15 vector components that contribute the most to these 2 principal components[4] the noisiest inputs are eliminated and the subsequent PCA yields a perfectly separable distribution (cf. figure 5).

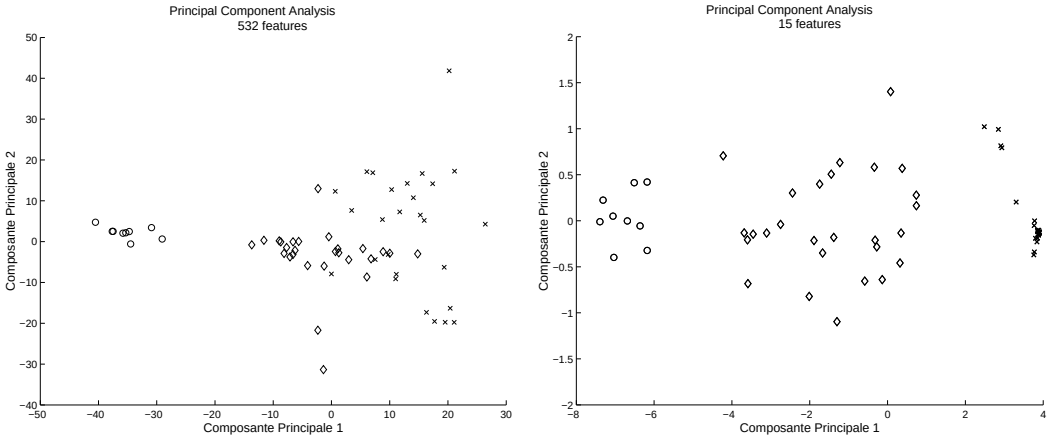

(a) (b)

Figure 5. Principal component analysis using (a) 532 features per vector and (b) the 15 most important components. Conforming parts are marked as (x), nonconforming parts due to a change of direction during brushing are marked as (o) and nonconforming parts due to faulty prepolishing are marked (⋄). The PCA using the 15 most important components affords a perfect separation of the three classes.

Because the 3 clusters in figure 5 are separable by vertical lines, the first principal component is sufficient to distinguish the different types of satin-finished parts.

To further test the relevance of the Optical Fourier features and in order to test the robustness of the classification, a

Kohonen neural network has been employed. A self-organized map was trained following a "leave-one-out" procedure.[1] For all 63 input vectors (7 parts x 9 measures) a vector is taken out and the network trained with the remaining ones. After the training the left out vector is used to verify if the network correctly classifies it. In this way an error rate can be established for the network and training database. In our case, a 3x3 self-organized map was tested and it produced a 100% classification rate.

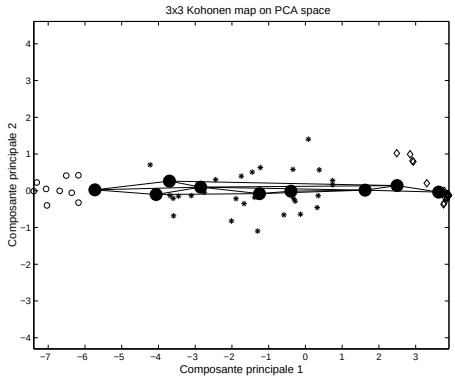

Figure 6. 3x3 Kohonen map projected on the PCA space. Conforming parts are marked as ($\diamond$), nonconforming parts due to a change of direction during brushing are marked as (o) and nonconforming parts due to faulty prepolishing are marked ($*$).

4. SCATTERING FEATURES

Metallic surfaces can be considered flat or rough depending on whether incident light is reflected in a diffusive or specular way. If the surface structure is of the same order of magnitude of the wavelength, Rayleigh scattering will occur.[13] Thus scattering is a common optical technique used in surface-roughness meters[14,15] and a whole conference is devoted to the subject.[16]

There are two types of scattering-based systems. Those that yield a scalar value, such as surface RMS or an intensity ratio between scattered and reflected light,[13] and those yielding a multidimensional measure, such as the scattered intensity along each angle, as in the angle-resolved scattering (ARS) devices.[17]

4.1. Setup

Since scalar-value measurements do not provide enough information to distinguish satin-finished parts –different surface states can have the same RMS– we have chosen to build an angle-resolved measurement device.

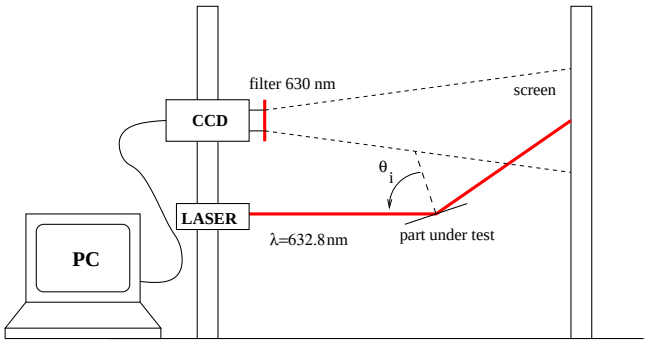

Figure 7. Setup for angle-resolved scattering for characterization of satin-finished surfaces.

The ARS setup has been built based on a grayscale, 8-bit CCD camera (figure 7). It consists of a 632 nm laser that projects a 10 mm^2 spot on the metallic surface with a high angle of incidence (60–70 degrees). Such an angle makes the subtended width of the grooves closer to the wavelength, which is a necessary condition for scattering to occur. The part is placed with the grooves parallel to the plane of incidence because it yields a concentrated scattering pattern that is easier to acquire with the CCD camera. The scattering pattern (cf. figure 8) is reflected on a screen and the CCD camera takes an image of it for further processing on the accompanying PC.

The scattering pattern forms an arc, the curvature of which depends on the angle of incidence and its thickness depends on the dispersion of the grating period around its average.[18]

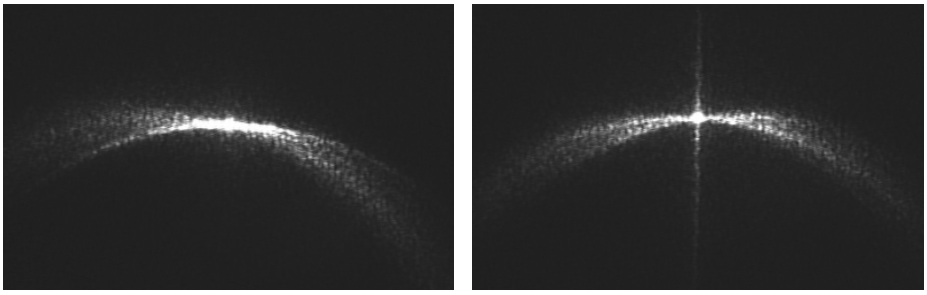

(a) (b)

Figure 8. Scattering pattern produced by reflection on a satin-finished part. (a) On a conforming part and (b) on a nonconforming part due to a nonuniform brushing direction.

4.2. Data

The same batch of parts described in section 3.3, consisting of 3 conforming and 4 nonconforming parts, has been analyzed. To this end 10 different zones per part have been measured using the setup described above.

For each image a circular regression has been used to render the measurement invariant to the curvature, i.e. the angle of incidence. Using the regression, the intensity profile along the curve is computed. Similarly, the intensity profile along a perpendicular line passing through the specular reflection spot is computed. Next, the following 5 features were extracted from the image (cf. figure 9):

- The average of the intensity profile along the circular regression.
- The average of the intensity profile along the perpendicular line.
- The size of the scattering pattern, defined as the number of pixels above a value of 15 and below a value of 60. Thanks to the filter in front of the camera the system is invariant to ambient illumination and absolute threshold values can be used.
- The size of the specular reflection spot, defined as the number of pixels above a value of 60.
- The dispersion (variance) of the scattering pattern around the circular regression. This feature is a measure of the "unstructuredness" of the satin-finished surface.

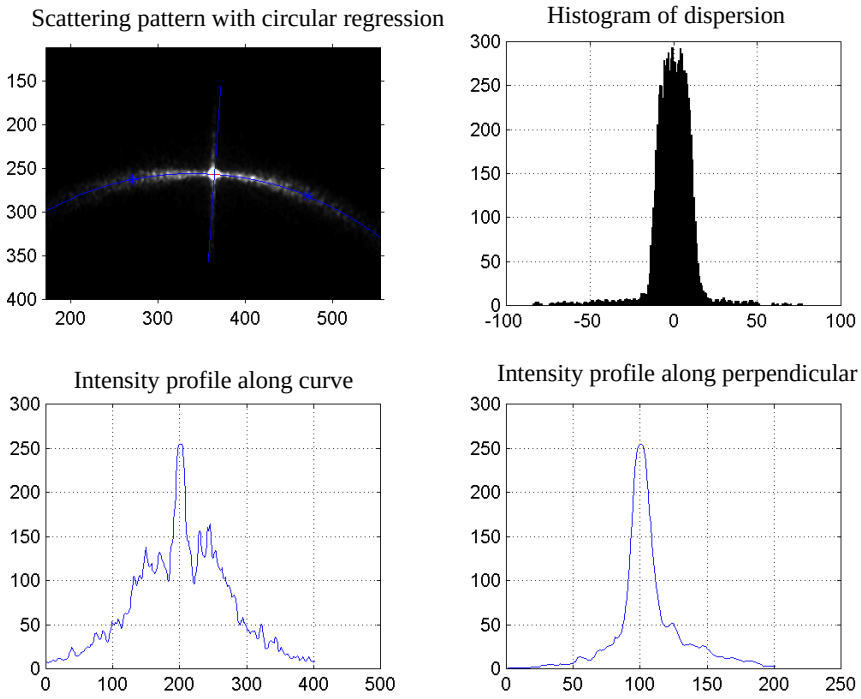

Figure 9. The features extracted from the image of a scattering pattern.

4.3. Results

A principal component analysis of the feature vectors described in section 4.2 has been carried out. The resulting PCA is shown in figure 10(a). Conforming parts are indicated by (□). Nonconforming parts are due to different assignable causes: (∗) imperfect prepolishing, (○) imperfect prepolish and nonuniform brushing direction, (+) brushing on uneven surface. Parts seem to be clearly clustered, affording a distinction between conforming and nonconforming parts. Furthermore, non conforming parts can be classified according to their assignable cause, thus affording to correct the process.

Classification can be further simplified by taking the two principal features, as indicated by the PCA. These are the average intensity along the perpendicular line and the size of the specular reflection spot. Figure 10(b) shows that these 2 features discriminate between conforming and nonconforming parts, but they cannot distinguish subclasses of nonconforming parts.

A 3x3 neuron LVQ classifier has also been applied on the data, obtaining a 96.6% classification rate after training for 1 epoch, where an epoch defines the number of times a feature is presented to the neural network. The robustness of the classification has been measured using the “leave-one-out” test with LVQ and yielding an average classification rate of 93.9%.

5. CONCLUSION

The two methods based on coherent light that have been presented –the optical Fourier transform and scattering– are shown to be capable of classifying satin-finished metallic parts according to the classes currently employed by human inspectors. For each of these methods, relevant features have been identified, particularly in the case of the scattering device.

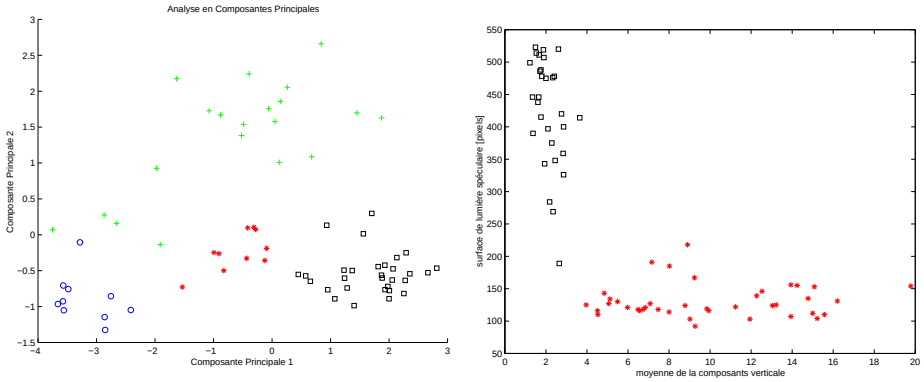

(a) Principal component analysis on (a) the five feature vectors defined in section 4.2. Conforming parts are indicated by (□). The remaining nonconforming parts are due to different assignable causes.

(b) Plot of the two principal features: average intensity along perpendicular line and size of specular reflection spot. These features are sufficient to distinguish conforming (∗) from nonconforming (□) parts.

Figure 10. PCA results on scattering features

These methods provide good discrimination among classes, as attested by the high classification rates (100% using PCA) and the robustness demonstrated with the leave-one-out test. The optical Fourier transform features yield more discriminant features than the scattering ones, but more samples would be needed to confirm this point.

Besides the capability of classifying satin-finished parts into the same classes currently employed by the human inspectors, the two methods provide 2 further advantages. By associating a number, or rather a vector to each part under inspection, they provide a quantitative, and hence objective, measurement that affords comparison across different operators and production lines. Such quantitative information affords the operators to impose, depending on the circumstances, more or less stringent conditions on the quality variability of the parts. Furthermore, by distinguishing different subclasses of nonconforming parts, assignable causes can be associated to each subclass, thus facilitating process improvement.

The two systems studied in this project are suitable for online inspection, as they can operate at frame-rate, 25 Hz. Indeed, they require acquiring a single image and the subsequent process, on 15- or 5-dimensional vectors, is simple vector algebra. Several such measurements per part would be needed to actually classify the part but the total time taken would still afford its use in production lines. Particularly so for manually-operated lines as in the luxury watchmaking industry.

As for the simplicity required for their use in a production environment, the scattering device is the most suitable one. Its only optical element is the camera objective, and it is not very sensible to positioning and orientation of the part under inspection. It is the most likely candidate for miniaturization and use as a portable device for online inspection by the manufacturing operators themselves.

Of course such a system would have to undergo a new training for each major change in production, such as a new brushing technique, or more particularly a different material or a different part shape.

5.1. Future work

The next steps to accomplish towards a production-line classification of metallic satin-finished surfaces using coherent light are threefold. The current classification is based on areas of approximately $10\,\mathrm{mm}^2$, but the parts are typically several square centimeters of surface. Since scanning the whole part would be too time-consuming, acceptance-sampling methodologies should be used to determine the number of samples per part that are necessary to classify it within a given confidence interval and the setup should be modified to position the part accordingly. Secondly, the classifiers should be

tested on a larger number of parts to be sure of their statistical relevance. And finally, the performance of the classifiers should be tested on rounded, satin-finished surfaces, that are the most common ones.

ACKNOWLEDGMENTS

We would like to thank Omar Sqalli of the IIOA–EPFL for his help with the OFT setup and optics theory in general. We acknowledge the contributions of Christoph Rüttimann and Tobias Kramer to the classification of satin-finished surfaces.

REFERENCES

1. S. Haykin, *Neural Networks: A Comprehensive Foundation*, Prentice Hall, 2^{nd} ed., 1998.
2. J. Jackson, "Principal components and factor analysis: part I," *Journal of Quality Technology* **12**, pp. 201–213, October 1980.
3. J. Jackson, "Principal components and factor analysis: part II," *Journal of Quality Technology* **13**, pp. 46–58, January 1981.
4. J. Cadima and I. Jolliffe, "Loading and correlation in the interpretation of principal components," *Journal of Applied Statistics* **22**, pp. 203–214, 1995.
5. T. Kohonen, *Self-Organizing Maps*, Springer, second edition ed., 1997.
6. Y. Linde, A. Buzo, and R. Gray, "An Algorithm for Vector Quantizer Design," *IEEE Transactions on Communications* **COM–28**, pp. 84–95, Jan 1980.
7. G. Meylan, "Conception d'un appareil portable de mesure d'etat de surface," tech. rep., LPM-IPR-EPFL, Lausanne, Switzerland, 2001.
8. J. Taboury, *Optique de Fourier, Première partie: Diffraction et imagérie cohérente*, Ecole Supérieure d'Optique, Paris, France, 1996.
9. J. Goodman, *Introduction to Fourier Optics*, McGraw-Hill, 2nd ed., 1996.
10. G. Zhang and Y. S., "Online measurement of the sizes of standard wire sieves using an optical fourier transform," *Optical Engineering* **39**(4), pp. 1098–1102, 2000.
11. M. Thomas, T. Day, and T. Kubo, "Application of fourier optical signal processing to detect surface flaws in transmissive and reflective materials," in *Proceedings of SPIE*, **680**, pp. 167–172, 1986.
12. G. Meylan, "Classification de surfaces métalliques satinées par l'analyse de la transformée de Fourier optique," tech. rep., LPM-IPR-EPFL, Lausanne, Switzerland, 2002.
13. J. Bennet and L. Mattson, *Introduction to surface roughness ans scattering*, Optical Society of America, Washington, 1989.
14. M. Ohlidal and M. Uncovsky, "Determination of the basic parameters characterizing the roughness of metal surfaces by laser light scattering," *Journal of Modern Optics* **46**(2), pp. 279–293, 1998.
15. J. Le Bosse, G. Hansali, J. Lopez, and J. Dumas, "Characterization of surface roughness by laser light scattering: diffusely scattered intensity measurement," *Wear* (224), pp. 236–244, 1999.
16. Z.-H. Gu and A. Maradudin, eds., *Scattering and surface roughness III*, (San Diego, California), SPIE, 2000.
17. A. Kasper and H. Rothe, "Evaluation of in-situ ARS sensors for characterizing smooth and rough surfaces," in *Scattering and surface roughness II*, pp. 252–261, SPIE, 1998.
18. F. Monay, "Analyse d'état de surface de pièces métalliques par scattering," tech. rep., LPM-IPR-EPFL, Lausanne, Switzerland, 2002.